Article:
Franks, P.J., Royer, D.L., Beerling, D.J. et al. (4 more authors) (2014) New constraints on atmospheric CO2 concentration for the Phanerozoic. Geophysical Research Letters, 41 (13). pp. 4685-4694. ISSN 0094-8276

https://doi.org/10.1002/2014GL060457

AGU PUBLICATIONS

Geophysical Research Letters

RESEARCH LETTER
10.1002/2014GL060457

Key Points:
- A novel CO_2 proxy calculates past atmospheric CO_2 with improved certainty
- CO_2 is unlikely to have exceeded ~1000 ppm for extended periods post Devonian
- Earth's long-term climate sensitivity to CO_2 is greater than originally thought

Supporting Information:
- Readme
- 2014GL060457_cs01.zip
- Text S1

Correspondence to:
P. J. Franks,
peter.franks@sydney.edu.au

Citation:
Franks, P. J., D. L. Royer, D. J. Beerling, P. K. Van de Water, D. J. Cantrill, M. M. Barbour, and J. A. Berry (2014), New constraints on atmospheric CO_2 concentration for the Phanerozoic, *Geophys. Res. Lett.*, *41*, 4685–4694, doi:10.1002/2014GL060457.

Received 8 MAY 2014
Accepted 23 JUN 2014
Accepted article online 25 JUN 2014
Published online 10 JUL 2014

New constraints on atmospheric CO_2 concentration for the Phanerozoic

Peter J. Franks[1], Dana L. Royer[2], David J. Beerling[3], Peter K. Van de Water[4], David J. Cantrill[5], Margaret M. Barbour[1], and Joseph A. Berry[6]

[1]Faculty of Agriculture and Environment, University of Sydney, Sydney, New South Wales, Australia, [2]Department of Earth and Environmental Sciences, Wesleyan University, Middletown, Connecticut, USA, [3]Department of Animal and Plant Sciences, University of Sheffield, Sheffield, UK, [4]Department of Earth and Environmental Sciences, California State University, Fresno, California, USA, [5]National Herbarium of Victoria, Royal Botanic Gardens Melbourne, South Yarra, Australia, [6]Department of Global Ecology, Carnegie Institution of Washington, Stanford, California, USA

Abstract Earth's atmospheric CO_2 concentration (c_a) for the Phanerozoic Eon is estimated from proxies and geochemical carbon cycle models. Most estimates come with large, sometimes unbounded uncertainty. Here, we calculate tightly constrained estimates of c_a using a universal equation for leaf gas exchange, with key variables obtained directly from the carbon isotope composition and stomatal anatomy of fossil leaves. Our new estimates, validated against ice cores and direct measurements of c_a, are less than 1000 ppm for most of the Phanerozoic, from the Devonian to the present, coincident with the appearance and global proliferation of forests. Uncertainties, obtained from Monte Carlo simulations, are typically less than for c_a estimates from other approaches. These results provide critical new empirical support for the emerging view that large (~2000–3000 ppm), long-term swings in c_a do not characterize the post-Devonian and that Earth's long-term climate sensitivity to c_a is greater than originally thought.

1. Introduction

Many basic features of Earth's pre-Quaternary paleoclimate history remain poorly characterized and understood, despite decades of research effort. Proxy methods and long-term carbon cycle models have identified periods of high atmospheric CO_2 concentration (c_a) that likely forced increases in global surface temperature and sea level [*Berner*, 2008; *Beerling and Royer*, 2011], but quantitative discrepancies and large or unbounded uncertainties surrounding these c_a estimates preclude confident assessment of Earth's climate sensitivity to c_a [*Royer et al.*, 2007; *Park and Royer*, 2011; *Royer et al.*, 2012]. Historically, reconstructions of c_a for the late Paleozoic, Mesozoic, and early Cenozoic greenhouse climates have been high (>2000 ppm) [*Royer et al.*, 2001; *Montanez et al.*, 2007; *Berner*, 2008], but re-evaluations of these records suggest more modest values (500–1000 ppm) [*Breecker et al.*, 2010; *Royer et al.*, 2012]. This revised c_a history implies a higher climate sensitivity to CO_2 [*Royer et al.*, 2012; *Hansen et al.*, 2013], but nearly all proxy-based c_a estimates for the pre-Cretaceous come from a single method based on carbonates in fossil soils (paleosols) that relies crucially on largely unknown soil respiration rates [*Ekart et al.*, 1999; *Breecker et al.*, 2010; *Cotton and Sheldon*, 2012]. New, independent, and well-constrained estimates of pre-Cretaceous c_a are urgently needed to better define Earth's long-term climate sensitivity to CO_2 [*Hansen et al.*, 2013].

The stomatal proxy method for estimating c_a in paleo-atmospheres exploits the negative correlation between stomatal density (*D*, number of stomata per unit leaf area) and the atmospheric CO_2 at which a plant grows, as observed in plant growth chamber experiments [*Woodward*, 1987]. The correlation has also been shown with *D* from herbaria material [*Woodward*, 1987] and fossil leaves, including Pleistocene and Holocene fossils, where c_a is known from ice cores [*Van de Water et al.*, 1994]. However, the shape of the relationship between *D* and c_a is specific to each "test" species, so using it quantitatively to reconstruct ancient c_a from the stomatal density of fossil leaves (or from the normalized equivalent of density, stomatal index [*Royer et al.*, 2001]) relies upon calibration using extant conspecifics. Therefore, estimates from this method are mostly limited to a few species that grew during the Late Cretaceous and Cenozoic and that persist to the present day. A further limitation is that the strong nonlinearity of the empirical calibrations propagates to unbounded upper error limits above c_a estimates of ~500–1000 ppm [*Royer et al.*, 2001], although the threshold for this effect is higher for some species [*Haworth et al.*, 2011]. A modified method based on the ratio of fossil stomatal density or index to nearest

ecological equivalent broadens the range of candidate taxa [*McElwain*, 1998], but estimates are considered semi-quantitative at best because the assumed linear scaling between stomatal ratio and the ratio of paleo- to present-day c_a is untested [*Royer et al.*, 2001].

Mechanistic models of leaf gas exchange are an increasingly viable alternative to traditional empirical methods in paleoclimate and paleoecology reconstructions [*Konrad et al.*, 2008; *Grein et al.*, 2011; *Roth-Nebelsick et al.*, 2014]. Here we estimate c_a across the Phanerozoic directly from fossil leaves with a new mechanistic approach that is largely free from the above restrictions and uncertainties.

2. Methods

2.1. Model Summary

We assume that photosynthetic gas exchange in past forests functioned under the same constraints as current forests, with the exception that c_a varied. Changes in c_a affect the rate of diffusion of CO_2 from the atmosphere to the sites of its fixation within the leaf, and this in turn affects the rate of biochemical fixation of CO_2. Extensive experimental investigations into leaf gas exchange have established the following fundamental biophysical model equating the concentration of CO_2 in the atmosphere, c_a (in μmol mol^{-1}), with the rate of CO_2 assimilation by leaves, A_n (in μmol m^{-2} s^{-1}) [*Farquhar and Sharkey*, 1982; *von Caemmerer*, 2000]:

$$c_a = \frac{A_n}{g_{c(tot)} \cdot (1 - c_i/c_a)}, \tag{1}$$

where $g_{c(tot)}$ is the total operational conductance to CO_2 diffusion from the atmosphere to sites of photosynthesis within the leaf (in mol m^{-2} s^{-1}) and c_i/c_a is the ratio of leaf internal CO_2 concentration (c_i) to c_a. An important physiological quality of the system described by equation (1) is that A_n, $g_{c(tot)}$, and c_i/c_a are interdependent, i.e., a change in one affects the others via feedback interactions that operate over short and long timescales [*Farquhar et al.*, 1978; *Buckley et al.*, 2003; *Franks et al.*, 2013].

2.2. Determining $g_{c(tot)}$

The total conductance to CO_2 from the atmosphere to sites of carboxylation within the leaf, $g_{c(tot)}$, comprises three main components in series: the leaf boundary layer conductance to CO_2, g_{cb}, the operational stomatal conductance, $g_{c(op)}$, and the mesophyll conductance, g_m. Operational stomatal conductance $g_{c(op)}$ is controlled by the plant at some point between approximately zero (closed stomata) and the maximum, $g_{c(max)}$, according to prevailing environmental conditions, and can be expressed conveniently as a fraction ζ of $g_{c(max)}$, i.e., $g_{c(op)} = \zeta g_{c(max)}$. For trees growing naturally under field conditions the mean ζ is typically around 0.2 [*Franks et al.*, 2009] (Table S1). The same ratio has also been found for a range of *Arabidopsis* genotypes with different stomatal patterning [*Dow et al.*, 2014]. The total conductance to CO_2 is therefore

$$g_{c(tot)} = \left(\frac{1}{g_{cb}} + \frac{1}{\zeta g_{c(max)}} + \frac{1}{g_m} \right)^{-1}. \tag{2}$$

Equation (2) is the standard form for hypostomatous leaves. For amphistomatous leaves the term $((1/g_{cb}) + (1/\zeta g_{c(max)}))^{-1}$ must be calculated separately for the upper (adaxial) and lower (abaxial) leaf surfaces, added together in parallel, and this then added in series with g_m to obtain $g_{c(tot)}$.

The number and size of stomata on leaves, including fossils, were measured to calculate $g_{c(max)}$. Stomatal size determines both the maximum stomatal aperture (a_{max}) and the depth (l) of the stomatal pore (Figure S2), with $g_{c(max)}$ given by the basic diffusion equation [*Franks and Beerling*, 2009]:

$$g_{c(max)} = \frac{d}{v} . D . a_{max} / \left(l + \frac{\pi}{2} \sqrt{a_{max}/\pi} \right), \tag{3}$$

where constants d and v are, respectively, the diffusivity of CO_2 in air and the molar volume of air, D is stomatal density, and a_{max} is approximated as a fraction β of a circle with diameter equal to the stomatal pore length p, i.e., $a_{max} = \beta(\pi p^2/4)$. Approximate values for β in broad groups of plants are given in Table S2, along with other useful geometric relationships. Over the long term (developmental to

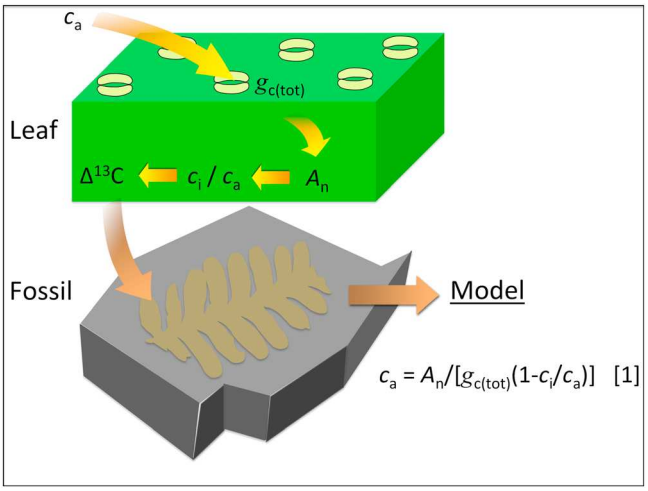

Figure 1. Plants as paleo-CO_2 sensors. During photosynthesis, CO_2 assimilation rate (A_n) is determined by the difference between atmospheric CO_2 concentration (c_a) and leaf internal CO_2 concentration (c_i) as well as the total stomatal conductance to CO_2, $g_{c(tot)}$ (see Methods). A physiological model equating c_a with A_n, $g_{c(tot)}$, and the ratio c_i/c_a (equation (1)) can be used to derive c_a at the time of photosynthesis. Central to this approach is the preservation in leaf fossils of the isotopic signal of carbon fixed during photosynthesis, $\Delta^{13}C$, from which an assimilation-weighted average value for c_i/c_a is easily derived (see equations (4) and (5)). Because A_n adapts to c_a (equation (6)), c_a is obtained by solving equations (1) and (6) simultaneously.

evolutionary timescales) leaves alter $g_{c(max)}$ by changing the density and/or size of stomata [*Franks and Beerling*, 2009; *Franks et al*., 2012]. These anatomical alterations increase or decrease $g_{c(max)}$, allowing $g_{c(op)}$ to be optimized for the new c_a [*Franks et al*., 2012].

2.3. Determining c_i/c_a

An estimate of the relative drawdown of CO_2 between the atmosphere and the sites of fixation (c_i/c_a) (see equation (1) and Figure 1) can be obtained by measurement of the relative carbon isotope composition, $\delta^{13}C$, of fossil leaves. The difference between the $\delta^{13}C$ of leaf carbon and that of its source in the atmosphere, $\delta^{13}C_{air}$, provides a measure of the carbon isotope discrimination by the plant, Δ_{leaf} (in parts per thousand, ‰) [*Farquhar et al*., 1989], and a theoretical relationship was used to relate this to the average c_i/c_a, weighted by the photosynthetic rate, over the time that the leaf grew [*Farquhar et al*., 1982]:

$$c_i/c_a = \left[\frac{\Delta_{leaf} - a}{b - a}\right] \quad (4)$$

where a is the carbon isotope fractionation due to diffusion of CO_2 in air (4.4‰) [*Farquhar et al*., 1982], b is the fractionation associated with RuBP carboxylase (taken here as 30‰) [*Roeske and O'Leary*, 1984], and Δ_{leaf} (‰) is given by [*Farquhar and Richards*, 1984]:

$$\Delta_{leaf} = \frac{\delta^{13}C_{air} - \delta^{13}C_{leaf}}{1 + \delta^{13}C_{leaf}/1000} \quad (5)$$

with $\delta^{13}C_{air}$ and $\delta^{13}C_{leaf}$ in units of ‰. The short-term feedback regulation of $g_{c(op)}$ tends to maintain c_i/c_a close to a relatively constant mean value [*Wong et al*., 1979; *Polley et al*., 1993; *Ehleringer and Cerling*, 1995]. This mechanism appears to hold also over long timescales [*Franks et al*., 2013].

2.4. Determining A_n

To estimate how A_n would have changed with long-term changes in c_a we apply the theory and rationale developed in *Franks et al*. [2013]. Briefly, in the Farquhar-von Caemmerer-Berry biochemical model for photosynthesis [*Farquhar et al*., 1980], $A_n = \min [W_e, W_c]$ where W_e is the light-limited rate and W_c is the Rubisco capacity-limited rate. The use of limiting protein resources is optimal when the protein is distributed in the chloroplast such that $W_c = W_e$ at the average light intensity that the leaf experiences during growth. Under typical conditions plants tend to operate near this point of transition [*Von Caemmerer and Farquhar*, 1981]. Assuming that adaptation over developmental to evolutionary timescales tends toward this optimal

condition, and that the average incident sunlight has not changed appreciably, we can use the expression for W_e alone (i.e., independently of W_c) to express how A_n will change as a function of c_a over long timescales. In the original biochemical model [*Farquhar et al*., 1980] the expression for W_e was given in terms of c_i, but acknowledging that A_n vs c_i and A_n vs c_a follow essentially the same curve, the same function can be used to describe the relationship between A_n and c_a relative to a given reference c_a (see *Franks et al*. [2013]). With this, and taking reference values for A_n and c_a under current ambient conditions as A_0 and c_{a0} respectively, then A_n for any given c_a was obtained from the expression [*Franks et al*., 2013]:

$$A_n \approx A_0 \left[\frac{(c_a - \Gamma^*)(c_{a0} + 2\Gamma^*)}{(c_a - 2\Gamma^*)(c_{a0} + \Gamma^*)}\right] \quad (6)$$

where Γ^* is the CO_2 compensation point in the absence of dark respiration. Although the CO_2 compensation point is influenced by leaf temperature [*Farquhar et al*., 1980] there is evidence to suggest that despite widely varying seasonal and latitudinal temperatures, much of the photosynthetic productivity of plants occurs within a relatively narrow band of leaf temperature ranging from about 19°C in boreal systems through to 26°C in tropical systems [*Helliker and Richter*, 2008; *Song et al*., 2011]. Applying this assumption, and acknowledging that plant fossil records are weighted toward temperate to tropical systems, we assume a mean leaf temperature during photosynthesis of 25°C, giving Γ^* a mean value of 40 μmol mol^{-1} as a first approximation for the Phanerozoic Eon.

2.5. Determining c_a

Assuming that over long geological time periods mean A_n is influenced by c_a (equation (6)), the calculation of c_a must address this interdependence. Our approach was to solve equations (1) and (6) simultaneously by iteration, giving c_a and A_n, after determining $g_{c(tot)}$ and c_i/c_a and all other physiological input variables independently from information in the fossil record and physiological data. Although long-term CO_2 manipulation experiments are not a perfect representation of geologic-scale processes, analysis of data from these experiments shows that plants generally adapt to CO_2 according to the trend predicted by equations (1) and (6) [*Franks et al*., 2013]. A computer program, written in "R," performed the iterative procedure and a full error propagation analysis via Monte Carlo simulations to obtain mean c_a with 16–84 percentile error. A fully interactive, user-friendly version of this program is available in the supporting information online. Further details on the parameterization of physiological input variables are given in the supporting information.

3. Results and Discussion

3.1. Model Boundaries and Sensitivity

We utilize the robust mathematical relationship between c_a, net CO_2 assimilation rate (A_n), total conductance to CO_2 ($g_{c(tot)}$), and leaf intercellular CO_2 concentration (c_i) (Figure 1, equation (1); see also Methods) [*Farquhar and Sharkey*, 1982]. Information preserved in the fossil record is used to derive c_i/c_a and $g_{c(tot)}$. The fractionation of carbon isotopes during photosynthesis causes the carbon products used to synthesize leaf tissue to be relatively depleted in the heavier ^{13}C isotope [*Farquhar et al*., 1989]. The assimilation-weighted average of this discrimination against ^{13}C, quantified as $\Delta^{13}C$ [*Farquhar et al*., 1989], is routinely measured in the carbon-based remains of plants preserved as fossils, such as the highly durable leaf cuticle [*Beerling et al*., 2002]. A correlation between $\Delta^{13}C$ and the ratio c_i/c_a during photosynthesis is described by a well-validated fractionation model (see Methods) [*Farquhar et al*., 1982], and this was used to determine c_i/c_a for fossil leaves. Additionally, to enable incorporation of stomatal data from extensive archives of published anatomical studies in which isotopes were not measured, we developed a regression model for c_i/c_a through the Phanerozoic from a compilation of Phanerozoic fossil plant $\delta^{13}C$ (Figure S1; $c_i/c_a = 0.6 - (6.4 \times 10^{-4})t + (8.9 \times 10^{-6})t^2 - (2.0 \times 10^{-8})t^3$, with t in Myr). The second of the fossil-derived terms, $g_{c(tot)}$, integrates the major diffusive conductances on each side of the leaf (see equation (2)).

We determined A_n based on the assumption that, over the very long term, plants optimize ribulose-1,5 bisphosphate (RuBP)-regeneration-limited photosynthesis for the prevailing incident light conditions [*Medlyn et al*., 2011; *Franks et al*., 2013], which we assume to be predominantly full sunlight [*Kürschner*, 1997]. The expression for RuBP-regeneration-limited photosynthesis as a function of c_a [*Farquhar et al*., 1980; *Franks*

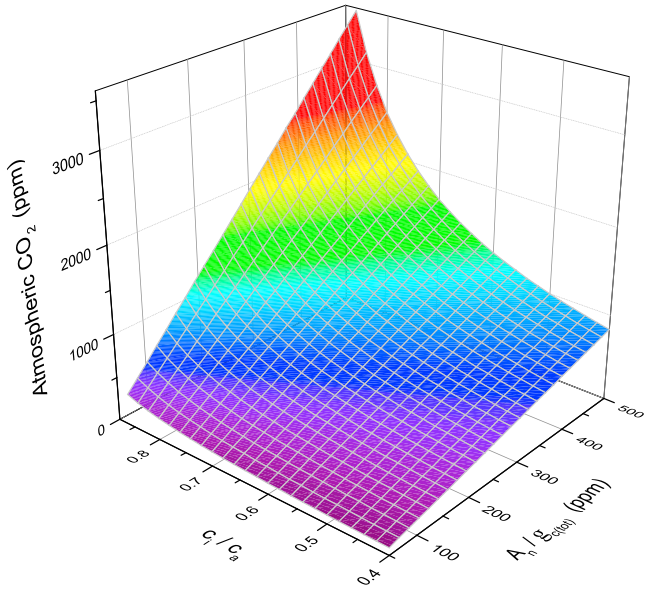

Figure 2. Model boundaries. Atmospheric CO_2 concentration (c_a) is shown for realistic combinations of c_i/c_a (ratio of leaf intercellular to ambient CO_2 concentration) and CO_2 drawdown from atmosphere to leaf interior (as determined by assimilation rate, A_n, divided by total conductance to CO_2, $g_{c(tot)}$).

et al., 2013] (see Methods) may therefore be used to describe the relative change in A_n with c_a over the long term. We emphasize that this is not a dynamic stomatal model that predicts instantaneous values; rather it uses the basic gas exchange equation and integrated mean typical values of its components, c_i/c_a, $g_{c(tot)}$, and A_n, to determine a mean typical c_a for those conditions. Because of the interdependence of A_n and c_a (Figure 1), equations (1)–(3) are solved simultaneously by iteration to yield c_a (see Methods). The limits of c_a estimated with our model are well bounded by the natural operating ranges of the key physiological variables A_n, $g_{c(tot)}$ and c_i/c_a (Figure 2).

We undertook a thorough analysis of errors in the c_a calculations by simultaneously propagating uncertainties in all input terms using Monte Carlo simulations (10,000 random samples) to characterize uncertainty in model behavior when applied to modern and fossil data sets. Standard errors of the mean (s.e.m.) were measured directly for stomatal dimensions (from which $g_{c(max)}$ is calculated), the ratio $g_{c(op)}/g_{c(max)}$, and the $\delta^{13}C$ of atmosphere and plant tissue (from which c_i/c_a is calculated). For the other variables and scaling factors we assigned mean values based on published data and assumed ±10% of the mean typically represented ±2 standard deviation [s.d.; *Schulze et al*., 1994; *Franks and Farquhar*, 1999]. Uncertainties in all input terms were modeled to behave in a Gaussian manner.

In comparison to other leading paleo-CO_2 proxies (see supporting information), our new approach is at least as accurate, with the advantage of being free from unbounded errors at high [*Royer et al*., 2001] or low [*Breecker et al*., 2010] c_a. Nonlinearity of the relationship between A_n and c_a (see Methods) results in larger absolute errors at higher c_a compared to lower c_a for any given error in the model input term $g_{c(tot)}$. However, these errors remain well constrained and are relatively consistent as a percentage of the mean c_a. To test the effects of additional error in the baseline values for A_0 and $g_{c(op)}/g_{c(max)}$, we ran the Monte Carlo simulations with ±20% as 2 standard deviations in these terms, and this resulted in little change (<3%) in the overall confidence interval of the model outputs.

3.2. Validation Against Modern CO_2 Measurements and Ice Cores

The method for calculating c_a was validated against independent measurements from three recent time periods. For comparison against current day c_a, $\Delta^{13}C$, stomatal anatomy, and A_0 were measured on living plants (Figure 3). In this case four extant species were chosen to represent a broad cross section of fossil plants: an angiosperm tree (*Quercus robur*) and four gymnosperms (*Sequoia sempervirens*, *Ginkgo biloba* and *Cycas revoluta*). The mean error in calculated current day c_a was within 2.6% (Figure 3, compare blue symbols with respect to blue reference line), which is comparable to three other leading CO_2 proxies (mean error rate = 8%, 12%, and 67% for the boron, alkenone, and paleosol carbonate methods; see supporting information). This is improved significantly when the data for all species are pooled, suggesting that CO_2 estimates may be more robust when multiple taxa are used for a given geological time. Model tests with an additional gymnosperm, *Wollemia nobilis,* grown in controlled environment chambers for 8 months at 480 and 1270 ppm atmospheric CO_2 yielded estimates of c_a that were within 7% of actual (Figure 3, compare yellow and red symbols from model output with yellow and red reference lines, respectively).

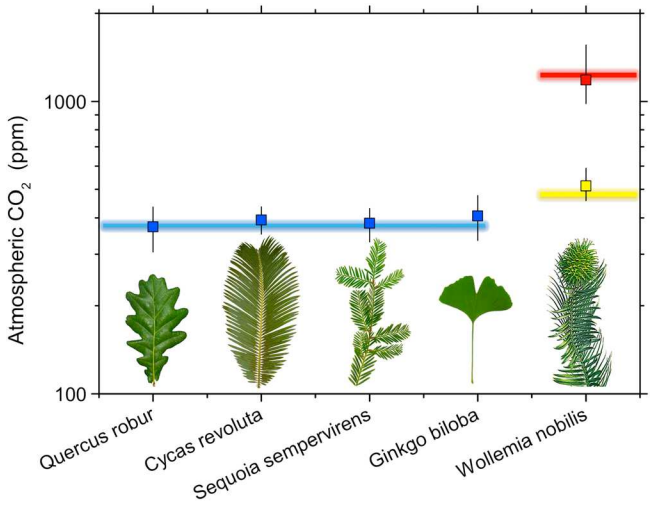

Figure 3. Model validation with extant species. Modeled c_a (symbols; error bars span 16–84 percentiles) closely matches the value of c_a in which the sample leaves grew (colored lines). Blue line represent current ambient atmospheric CO_2 concentration in which *Quercus robur*, *Cycas revoluta*, *Sequoia sempervirens*, and *Ginkgo biloba* were growing under natural conditions outdoors; yellow and red lines represent, respectively, 480 and 1270 ppm atmospheric CO_2 concentration inside controlled environment chambers where *Wollemia nobilis* was grown.

For comparison against the Anthropocene rise in c_a measured between 1958 and 1992 at the Mauna Loa observatory (Figure 4a) and in ice cores representing the c_a spanning the Pleistocene-Holocene transition approximately 2–27 kyr before present (Figure 4b), we used measurements of $\Delta^{13}C$ and stomatal anatomy in naturally preserved leaf material [*Wagner et al.*, 1996; *Van de Water et al.*, 1994]. Calculated c_a for the period 1958–1992 closely tracks the steady rise in c_a measured at Mauna Loa (Figure 4a). For the Pleistocene-Holocene transition, modeled c_a reproduces the sudden rise at ~15–12 kyr before present (Figure 4b). The slight positive offset in the modeled Pleistocene mean c_a (12–27 kyr before present, Figure 4b) is removed by applying a −10% correction to A_0 to account for the ~1°C lower July growing season temperature in the Great Basin area at this time [*Reinemann et al.*, 2009]. However, this effect is sufficiently accommodated in the ±10% error assigned to A_0, noting that in Figure 4b the ice core c_a values are mostly within the errors for modeled c_a. For individual taxa, when input terms are based on well-replicated measurements (s.e.m ~5–10% of mean), the 95% confidence interval obtained by Monte Carlo simulations of error propagation is generally within −25% to +35% of the median CO_2 estimate (see also Figures 4a–4c).

To further test the model beyond the limits of verification by ice core records, we used $\delta^{13}C$ and stomatal dimensions from [*Kürschner et al.*, 1996] to calculate c_a for the late Neogene to early Pleistocene (~10–2 Myr ago; Figure 4c). In terms of accuracy, the calculated mean c_a values are remarkably similar to those in [*Kürschner et al.*, 1996], where stomatal index was used as a proxy for c_a. Note that in this case the errors are not comparable due to different error calculation methodologies. The results show c_a to be relatively stable between ~280 and 370 ppm, with low values at approximately 6.4 and 4.4 Myr ago. These estimates are consistent also with those from other proxy methods [*Beerling and Royer*, 2011], except that marine alkenone and boron proxies show c_a peaking close to 500 ppm from about 3 to 6 Myr ago [*Seki et al.*, 2010].

3.3. Phanerozoic CO_2

Calculated c_a is below 1000 ppm for most of the Phanerozoic, from the Devonian onwards (Figure 4d, red symbols). Overall, the trend in Phanerozoic c_a follows that of the GEOCARBSULFvolc long-term carbon cycle model (Figure 4d, black line), except for the late Mesozoic (~140 Myr ago) where the fossil model yields somewhat lower c_a. The highest c_a since the Devonian occurs during the Mesozoic greenhouse interval (~240–60 Myr ago) while c_a is at its lowest, near current day values, during the glacial intervals of the late Paleozoic (~300 Myr ago) and late Cenozoic (last 34 Myr). Fluctuations in atmospheric O_2 throughout the Phanerozoic would have had a small influence on CO_2 assimilation rate, but the effect of this on the c_a estimates, including the biggest excursion in O_2 around the Carboniferous-Permian transition [*Berner et al.*, 2007], is accounted for both through its effects on leaf c_i/c_a ratios [*Beerling et al.*, 2002] and in the model through the ±10% error assigned to A_0. Moreover, elevated O_2 lowers the estimates of CO_2, reinforcing our general conclusion of $<$1000 ppm CO_2.

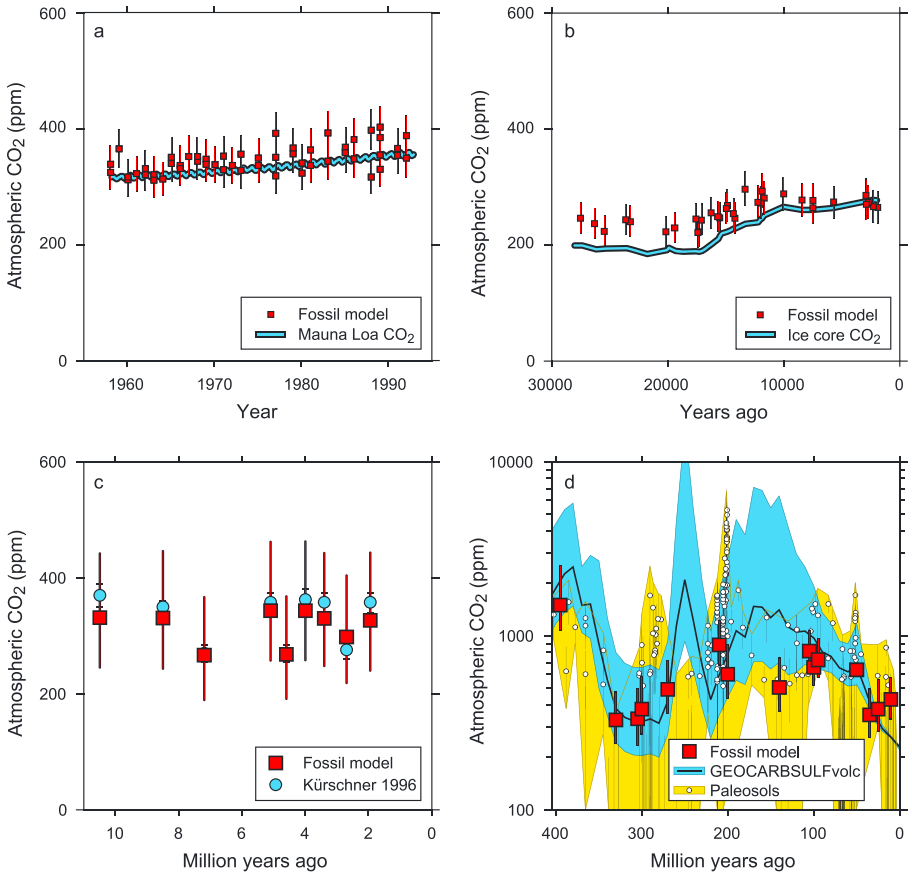

Figure 4. Atmospheric CO_2 concentration, c_a, calculated for different geological timescales. All red symbols are c_a values calculated from fossil leaves (or, for panel a, leaves preserved in peat). Error bars on red symbols span 16–84 percentiles (similar to ±1 σ), unless noted otherwise. (a) Validation against direct measurements of c_a (blue line) at Mauna Loa observatory, Hawaii, from 1958 to 1994 [*Tans and Keeling*, 2012], using leaf information for *Betula pendula* from *Wagner et al.* [1996]; (b) validation against measurements of c_a from ice cores [*Smith et al.*, 1999; *Monnin et al.*, 2004) (blue line) for 27–2 kyr before present, showing the Pleistocene-Holocene transition, using fossil information for *Pinus flexilis* from *Van de Water et al.* [1994]; (c) comparison with stomatal index-based estimates [*Kürschner et al.*, 1996] (blue symbols; associated bars represent s.e.m.) for ~10– 2 Myr before present, using fossil information for *Quercus petraea* in *Kürschner et al.* [1996]; error bars represent 18 and 84 percentiles to allow better comparison with the stomatal index-based estimates; (d) c_a modeled using fossil information for multiple species from published studies (see Table S7), compared with estimates from GEOCARBSULFvolc (black line; 10–90 percentile error in blue; [*Berner*, 2008; *Royer et al.*, 2007]) and paleosol carbonate (updated from *Park and Royer* [2011]; error envelope in yellow). Paleosol estimates are revised with downward-corrected soil respiration term $S(z)$ following *Breecker et al.* [2010]. For paleosol estimates under 500 ppm, only the error ranges are plotted, in keeping with the general loss of precision of this method at low CO_2.

Overall, errors are better constrained across the Phanerozoic in the fossil model than in GEOCARBSULFvolc and the revised (downward-corrected soil respiration term $S(z)$ [*Breecker et al.*, 2010]) paleosol carbonate proxy (Figure 4d; compare height of the blue and yellow bands with hash marks on red symbols) and—especially at high c_a— traditional stomatal approaches [*Royer et al.*, 2007]. These errors will improve in future applications of the fossil model where c_i/c_a is calculated from direct measurements of plant $\delta^{13}C$ rather than using the regression model, reducing the standard error of estimated c_i/c_a.

Our results highlight a fundamental transition in Earth's atmosphere following the evolution of forests in the mid Devonian (~390 Myr ago) [*Stein et al.*, 2012]. Up until this point, according to both the GEOCARBSULFvolc and fossil models, c_a exceeded 1000 ppm. However, for the remainder of the Phanerozoic c_a was less than 1000 ppm, consistent with the emergence of global forests that captured and sequestered vast amounts of carbon from the atmosphere [*Berner*, 2003]. Forests also enhanced silicate mineral weathering, further removing CO_2 from the atmosphere via the deposition of carbonates in deep ocean sediments [*Berner*, 2003]. We emphasize that our low-resolution record bears most directly on long-term fluctuations in atmospheric CO_2;

we cannot exclude the possibility for short-term CO_2 excursions exceeding 1000 ppm, for example during the mass extinction at the Triassic-Jurassic (T-J) transition ~201 Myr ago [*McElwain et al*., 1999; *Steinthorsdottir et al*., 2011].

Our new Phanerozoic CO_2 record provides critical empirical support for the view that c_a has largely remained under 1000 ppm since the Devonian (the last ~350 Myr) [*Breecker et al*., 2010]. Until now, this view was based mainly on reanalysis of c_a estimates from the isotopic composition of carbonates in paleosols, the only extensive proxy record to span most of the Phanerozoic. Compared with the revised paleosol record (Figure 4d, yellow envelope) our calculations of Phanerozoic c_a produce similar mean values but with less uncertainty, although adjusting the S(z) correction to account for different soil orders could improve the uncertainty in the paleosol record (see supporting information).

It emerges that long-term atmospheric CO_2 concentration since the Devonian is constrained between the lower and upper limits of ~200 to 1000 ppm, possibly via strong negative feedbacks in the geochemical carbon cycle. Terrestrial plants may play a central role in this process. Stabilization of c_a at the lower limit of 200–250 ppm during the past 24 Myr appears to result from a strong negative feedback in the form of attenuation of silicate rock weathering as terrestrial vegetation approaches CO_2 starvation [*Pagani et al*., 2009]. Conversely, accelerated silicate weathering at elevated atmospheric CO_2 may be a dominant negative feedback helping to keep c_a below 1000 ppm.

These new constraints on Phanerozoic c_a will greatly assist in establishing benchmarks for Earth system sensitivity to CO_2 (also known as "slow-feedback" or "long-term" climate sensitivity). If peak Phanerozoic c_a is of the order of 1000 ppm then either slow-feedback climate sensitivity is greater than the canonical fast-feedback value of 3°C for $2 \times CO_2$ [*Solomon et al*., 2007], or global temperatures have been no warmer than ~6°C above preindustrial conditions. The latter possibility is at odds with most paleotemperature records [*Schouten et al*., 2003; *Tripati et al*., 2003; *Pearson et al*., 2007; *Littler et al*., 2011; *Royer et al*., 2012]. As we face a potential doubling or tripling of c_a from its preindustrial value by the end of this century [*Solomon et al*., 2007], a long-term climate sensitivity exceeding 3°C for CO_2 doubling has important ramifications for a range of critical global economic, social, and political issues [*Hansen et al*., 2013]. The possibility of higher climate sensitivity to CO_2 in the face of inevitable increases in atmospheric CO_2 concentration should be considered within the framework of climate adaptation policy.

Acknowledgments

We thank the ARC and conveners of the ARC-NZ Network for Vegetation Function, Mark Westoby and Ian Wright, and gratefully acknowledge assistance from F. Wagner-Cremer (Utrecht University) who provided data from [*Wagner et al*., 1996] for use in Figure a, and W.M. Kürschner (University of Oslo) who provided data from *Kürschner et al*. [1996] for use in Figure c. Data used to generate all figures are available from the corresponding author upon request.

The Editor thanks two anonymous reviewers for their assistance in evaluating this paper.

References

Beerling, D. J., and D. L. Royer (2011), Convergent Cenozoic CO_2 history, *Nat. Geosci.*, *4*, 418–420.

Beerling, D. J., J. A. Lake, R. A. Berner, L. J. Hickey, D. W. Taylor, and D. L. Royer (2002), Carbon isotope evidence implying high O_2/CO_2 ratios in the Permo-Carboniferous atmosphere, *Geochim. Cosmochim. Acta*, *66*, 3757–3767.

Berner, R. (2008), Addendum to "Inclusion of the weathering of volcanic rocks in the Geocarbsulf Model" (R. A. Berner, 2006, V. 306, P. 205–302), *Am. J. Sci.*, *308*, 100–103.

Berner, R. A. (2003), The long-term carbon cycle, fossil fuels and atmospheric composition, *Nature*, *426*, 323–326.

Berner, R. A., J. M. Vandenbrooks, and P. D. Ward (2007), Oxygen and evolution, *Science*, *316*, 557–558.

Breecker, D. O., Z. D. Sharp, and L. D. Mcfadden (2010), Atmospheric CO_2 concentrations during ancient greenhouse climates were similar to those predicted for A.D. 2100, *Proc. Natl. Acad. Sci. U.S.A.*, *107*, 576–580.

Buckley, T. N., K. A. Mott, and G. D. Farquhar (2003), A hydromechanical and biochemical model of stomatal conductance, *Plant Cell Environ.*, *26*, 1767–1785.

Cotton, J. M., and N. D. Sheldon (2012), New constraints on using paleosols to reconstruct atmospheric pCO_2, *Geol. Soc. Am. Bull.*, *124*, 1411–1423.

Dow, G. J., D. C. Bergmann, and J. A. Berry (2014), An integrated model of stomatal development and leaf physiology, *New Phytol.*, *210*, 1218–1226.

Ehleringer, J. R., and T. E. Cerling (1995), Atmospheric CO_2 and the ratio of intercellular to ambient CO_2 concentrations in plants, *Tree Physiol.*, *15*, 105–111.

Ekart, D. D., T. E. Cerling, I. P. Montanez, and N. J. Tabor (1999), A 400 million year carbon isotope record of pedogenic carbonate: Implications for paleoatmospheric carbon dioxide, *Am. J. Sci.*, *299*, 805–827.

Farquhar, G. D., and R. A. Richards (1984), Isotopic composition of plant carbon correlates with water-use-efficiency of wheat genotypes, *Aust. J. Plant Physiol.*, *11*, 539–552.

Farquhar, G. D., and T. D. Sharkey (1982), Stomatal conductance and photosynthesis, *Ann. Rev. Plant Physiol.*, *33*, 17–45.

Farquhar, G. D., D. R. Dubbe, and K. Raschke (1978), Gain of the feedback loop involving carbon dioxide and stomata. Theory and measurement, *Plant Physiol.*, *62*, 406–412.

Farquhar, G. D., S. Von Caemmerer, and J. A. Berry (1980), A biochemical model of photosynthetic CO_2 assimilation in leaves of C_3 plants, *Planta*, *149*, 78–90.

Farquhar, G. D., M. H. O'leary, and J. A. Berry (1982), On the relationship between carbon isotope discrimination and the intercellular carbon dioxide concentration in leaves, *Aust. J. Plant Physiol.*, *9*, 121–137.

Farquhar, G. D., J. R. Ehleringer, and K. T. Hubick (1989), Carbon isotope discrimination and photosynthesis, *Ann. Rev. Plant Phys.*, *40*, 503–537.

Franks, P. J., and D. J. Beerling (2009), Maximum leaf conductance driven by CO_2 effects on stomatal size and density over geologic time, *Proc. Natl. Acad. Sci. U.S.A.*, *106*, 10,343–10,347.
Franks, P. J., and G. D. Farquhar (1999), A relationship between humidity response, growth form and photosynthetic operating point in C_3 plants, *Plant Cell Environ.*, *22*, 1337–1349.
Franks, P. J., P. L. Drake, and D. J. Beerling (2009), Plasticity in maximum stomatal conductance constrained by negative correlation between stomatal size and density: An analysis using *Eucalyptus globulus*, *Plant Cell Environ.*, *32*, 1737–1748.
Franks, P. J., I. J. Leitch, E. M. Ruszala, A. M. Hetherington, and D. J. Beerling (2012), Physiological framework for adaptation of stomata to CO_2 from glacial to future concentrations, *Philos. Trans. Roy. Soc. B*, *367*, 537–546.
Franks, P. J., et al. (2013), Sensitivity of plants to changing atmospheric CO_2 concentration: From the geological past to the next century, *New Phytol.*, *197*, 1077–1094.
Grein, M., W. Konrad, V. Wilde, T. Utescher and A. Roth-Nebelsick (2011) Reconstruction of atmospheric CO_2 during the early middle Eocene by application of a gas exchange model to fossil plants from the Messel Formation, Germany, *Palaeogeogr. Palaeoclimatol. Palaeoecol.*, *309*, 383–391.
Hansen, J., M. Sato, G. Russell, and K. Pushker (2013), Climate sensitivity, sea level, and atmospheric CO_2, *Philos. Trans. R. Soc. A*, *371*, 20120294, doi:10.1098/rsta.2012.0294.
Haworth, M., C. Elliott-Kingston, and J. C. McElwain (2011), The stomatal CO_2 proxy does not saturate at high atmospheric CO_2 concentration: Evidence from stomatal index responses of Araucariaceae conifers, *Oecologia*, *167*, 11–19.
Helliker, B. R., and S. L. Richter (2008), Subtropical to boreal convergence of tree-leaf temperatures, *Nature*, *454*, 511–514.
Konrad, W., A. Roth-Nebelsick, and M. Grein (2008), Modelling of stomatal density response to atmospheric CO_2, *J. Theor. Biol.*, *253*, 638–658.
Kürschner, W. A., J. Van Der Burgh, E. H. Visscher, and D. Dilcher (1996), Oak leaves as biosensors of late Neogene and early Pleistocene paleoatmospheric CO_2 concentrations, *Mar. Micropaleontol.*, *27*, 299–312.
Kürschner, W. M. (1997), The anatomical diversity of recent and fossil leaves of the durmast oak (*Quercus petraea* Lieblein/*Q. pseudocastanea* Goeppert)—Implications for their use as biosensors of palaeoatmospheric CO_2 levels, *Rev. Palaeobot. Palynol.*, *96*, 1–30.
Littler, K., S. A. Robinson, P. R. Brown, A. J. Nederbragt, and R. D. Pancost (2011), High sea-surface temperatures during the Early Cretaceous Epoch, *Nat. Geosci.*, *4*, 169–172.
Mcelwain, J. C. (1998), Do fossil plants signal palaeoatmospheric carbon dioxide concentration in the geological past?, *Philos. Trans. R. Soc. B*, *353*, 83–96.
Mcelwain, J. C., D. J. Beerling, and F. I. Woodward (1999), Fossil plants and global warming at the Triassic-Jurassic boundary, *Science*, *285*, 1386–1390.
Medlyn, B. E., R. A. Duursma, D. Eamus, D. S. Ellsworth, I. C. Prentice, C. V. M. Barton, K. Y. Crous, P. De Angelis, M. Freeman, and L. Wingate (2011), Reconciling the optimal and empirical approaches to modelling stomatal conductance, *Global. Change Biol.*, *17*, 2134–2144.
Monnin, E., et al. (2004), EPICA Dome C ice core high resolution Holocene and Transition CO_2 data, IGBP PAGES/World Data Center for Paleoclimatology, Data Contribution Series # 2004–055, NOAA/NGDC Paleoclimatology Program, Boulder, Colo.
Montanez, I. P., N. J. Tabor, D. Niemeier, W. A. Dimichele, T. D. Frank, C. R. Fielding, J. L. Isbell, L. P. Birgenheier, and M. C. Rygel (2007), CO_2-forced climate instability during late Paleozoic deglaciation, *Science*, *315*, 87–91.
Pagani, M., K. Caldeira, R. Berner, and D. J. Beerling (2009), The role of terrestrial plants in limiting atmospheric CO_2 decline over the past 24 million years, *Nature*, *460*, 85–88.
Park, J., and D. L. Royer (2011), Geologic constraints on the glacial amplification of Phanerozoic climate sensitivity, *Am. J. Sci.*, *311*, 1–26.
Pearson, P. N., B. E. van Dongen, C. J. Nicholas, R. D. Pancost, S. Schouten, J. M. Singano, and B. S. Wade (2007), Stable warm tropical climate through the Eocene Epoch, *Geology*, *35*, 211–214.
Polley, H. W., H. B. Johnson, B. D. Marino, and H. S. Mayeux (1993), Increase in C_3 plant water-use efficiency and biomass over Glacial to present CO_2 concentrations, *Nature*, *361*, 61–64.
Reinemann, S. A., D. F. Porinchu, A. M. Bloom, B. G. Mark, and J. E. Box (2009), A multi-proxy paleolimnological reconstruction of Holocene climate in the Great Basin, *Quat. Res.*, *72*, 347–358.
Roeske, C. A., and M. H. O'leary (1984), Carbon isotope effects on the enzyme-catalyzed carboxylation of ribulase bisphosphate, *Biochem.-US*, *23*, 6275–6284.
Roth-Nebelsick, A., C. Oehm, M. Grein, T. Utescher, L. Kunzmann, J.-P. Friedrich, and W. Konrad (2014), Stomatal density and index data of *Platanus neptuni* leaf fossils and their evaluation as a CO_2 proxy for the Oligocene, *Rev. Palaeobot. Palynol.*, *206*, 1–9.
Royer, D. L., R. A. Berner, and D. J. Beerling (2001), Phanerozoic atmospheric CO_2 change: Evaluating geochemical and paleobiological approaches, *Earth Sci. Rev.*, *54*, 349–392.
Royer, D. L., R. A. Berner, and J. Park (2007), Climate sensitivity constrained by CO_2 concentrations over the past 420 million years, *Nature*, *446*, 530–532.
Royer, D. L., M. Pagani, and D. J. Beerling (2012), Geobiological constraints on Earth system sensitivity to CO_2 during the Cretaceous and Cenozoic, *Geobiology*, *10*, 298–310.
Schouten, S., E. C. Hopmans, A. Forster, Y. van Breugel, M. M. M. Kuypers, and J. S. S. Damsté (2003), Extremely high sea-surface temperatures at low latitudes during the middle Cretaceous as revealed by archaeal membrane lipids, *Geology*, *31*, 1069–1072.
Schulze, E.-D., F. M. Kelliher, C. Korner, J. Lloyd, and R. Leuning (1994), Relationships among maximum stomatal conductance, carbon assimilation rate, and plant nutrition, *Annu. Rev. Ecol. Syst.*, *25*, 629–660.
Seki, O., G. L. Foster, D. N. Schmidt, A. Mackensen, K. Kawamura, and R. D. Pancost (2010), Alkenone and boron-based Pliocene pCO_2 records, *Earth Planet. Sci. Lett.*, *292*, 210–211.
Smith, H. J., H. Fischer, M. Wahlen, D. Mastroianni, and B. Deck (1999), Dual modes of the carbon cycle since the Last Glacial Maximum, *Nature*, *400*, 248–250.
Solomon, S., D. Quin, M. Manning, Z. Chen, M. Marquis, K. B. Averyt, M. Tignor, and H. L. Miller (Eds.) (2007), *Climate Change 2007: The Physical Basics. Contribution of Working Group I to the Fourth Assessment Report of the Intergovernmental Panel on Climate Change*, Cambridge Univ. Press, Cambridge, U. K.
Song, X., M. M. Barbour, M. Saurer, and B. R. Helliker (2011), Examining the large-scale convergence of photosynthesis-weighted tree leaf temperatures through stable oxygen isotope analysis of multiple data sets, *New Phytol.*, *192*, 912–924.
Stein, W. E., C. M. Berry, L. V. Hernick, and F. Mannolini (2012), Surprisingly complex community discovered in the mid-Devonian fossil forest at Gilboa, *Nature*, *483*, 78–81.
Steinthorsdottir, M., A. J. Jeram, and J. C. McElwain (2011), Extremely elevated CO_2 concentrations at the Triassic/Jurassic boundary, *Palaeogeogr. Palaeoclimatol. Palaeoecol.*, *308*, 418–432.

Tans, P., and R. Keeling (2012), Mauna Loa CO_2 annual mean data, U.S. National Oceanic and Atmospheric Administration, Earth System Research Laboratory, Boulder, Colo. [Available at http://www.esrl.noaa.gov/gmd/ccgg/trends/mlo.html.]

Tripati, A., M. L. Delaney, J. C. Zachos, L. D. Anderson, D. C. Kelly, and H. Elderfield (2003), Tropical sea-surface reconstruction for the early Paleogene using Mg/Ca ratios of planktonic foraminifera, *Paleoceanography*, *18*(4), 1101, doi:10.1029/2003PA000937.

Van de Water, P. K., S. W. Leavitt, and J. L. Betancourt (1994), Trends in stomatal density and $^{13}C/^{12}C$ ratios of *Pinus flexilis* needles during last glacial-interglacial cycle, *Science*, *264*, 239–243.

Von Caemmerer, S. (2000), *Biochemical Models of Leaf Photosynthesis*, CSIRO Publishing, Collingwood, Vic., Australia.

Von Caemmerer, S., and G. D. Farquhar (1981), Some relationships between the biochemistry of photosynthesis and the gas exchange of leaves, *Planta*, *153*, 376–387.

Wagner, F., R. Below, P. De Klerk, D. L. Dilcher, H. Joosten, W. A. Kurschner, and E. H. Visscher (1996), A natural experiment on plant acclimation: Lifetime stomatal frequency response of an individual tree to annual atmospheric CO_2 increase, *Proc. Natl. Acad. Sci. U.S.A.*, *93*, 11,705–11,708.

Wong, S. C., I. R. Cowan, and G. D. Farquhar (1979), Stomatal conductance correlates with photosynthetic capacity, *Nature*, *282*, 424–426.

Woodward, F. I. (1987), Stomatal numbers are sensitive to increases in CO_2 from preindustrial levels, *Nature*, *327*, 617–618.